OAK RIDGE NATIONAL LABORATORY
operated by
UNION CARBIDE CORPORATION
NUCLEAR DIVISION
for the
U.S. ATOMIC ENERGY COMMISSION

ORNL - TM - 2423

COPY NO. - 46

DATE - December 18, 1968

Neutron Physics Division

COMPARISON OF MONTE CARLO CALCULATIONS WITH MEASUREMENTS OF FAST-NEUTRON DOSE TRANSMITTED FROM A BEAM SOURCE THROUGH A SNAP-2 LiH SHIELD

V. R. Cain and K. D. Franz*

Abstract

Measurements and calculations were made of fast-neutron dose rates transmitted through a LiH SNAP shield surrounded by a collar shield of iron and oil. This was done in order to evaluate the Monte Carlo techniques used to design the experimental configurations for SNAP shielding experiments at the Tower Shielding Facility. Comparisons were made for a number of typical configurations and the calculated and measured fast-neutron dose rates for neutrons leaving both the LiH shield and the collar shield are in excellent agreement. This establishes the validity of this technique for analyzing future experiments.

*Computing Technology Center

I. INTRODUCTION

The forthcoming experimental program to be conducted at the Tower Shielding Facility (TSF) using a modified SNAP-10A reactor, the TSF-SNAP, has as one of its requirements measurements that can be related to the fast-neutron dose at the dose plane of an instrumented SNAP system, as it would exist in flight. These data cannot, of course, be obtained directly on earth because of structure and ground scattering. Preliminary calculations[1] indicated that it would be feasible to perform the measurements with a collimated detector and a collar surrounding the SNAP LiH shield to block the air-scattered neutrons. For the measurement to be obtained with high accuracy, the collar should be designed so as to give minimum perturbation to the ideal measurement, and whatever perturbation does exist should be known with high accuracy. The amount of the perturbation must, of course, be obtained by calculation.

An experiment[2] was conducted at the TSF with beams of radiation from the TSR-II and a SNAP-2 LiH shield, with the following objectives:

1. to determine whether cracks existed in the cast LiH shield,
2. to determine experimentally, insofar as possible, the relative effectiveness of different collar configurations,
3. to provide data to verify Monte Carlo calculations, which were to be used to determine the final collar design and to determine the collar perturbation.

This report describes the transformations of the experimental data to a form suitable for comparison, the calculational techniques used, and comparison of the calculated and experimental data.

Several manipulations of the raw data[2] were required to permit easy comparison with the Monte Carlo calculations. The first step was to subtract backgrounds from foregrounds for all modified long counter (MLC) results. The MLC count rates were then normalized so as to agree with the fast-neutron dosimeter (FND) results. The normalization was done by multiplying the MLC count rates by the mean ratio of FND dose results to MLC count rates (1.26×10^{-5} $ergs \cdot gm^{-1} \cdot hr^{-1}/cpm$ with a standard deviation of about 0.028×10^{-5}). Differences of these equivalent FND data were then taken to obtain the neutron dose at the detector due only to neutrons leaving the LiH shield surface, and due only to neutrons leaving the collar shield surface. The former is obtained by subtracting results obtained with a 12-in. polyethylene shield behind the LiH shield (subtending only the LiH shield surface, as seen from the detector) from the results with no shadow shield. The latter quantity is obtained by subtracting results obtained with a 19-in. water tank covering both the LiH and collar shields from the results obtained with the 12-in. polyethylene shield. The resulting data are presented in Table I (derived from the data in Tables 1, 3, 4, and 5 in ref. 2).

The last necessary quantity derived from the experimental data was the total dose incident on the LiH shield. This was obtained by numerically integrating the results of the direct-beam mapping (Table 7, ref. 2) by the FND in its air-scattered shield. This result was 168.6 $erg \cdot gm^{-1} \cdot hr^{-1} \cdot w^{-1} \cdot cm^{2}$.

II. TECHNIQUES

The Monte Carlo calculations were made using O5R,[3] a general-purpose neutron transport code, and ACTIFK,[4] a general analysis code for O5R. Supplied to O5R with each calculation were the geometry of the shield and one of three possible geometries for the collar: a source description, the reactions taking place in the system, and special biasing parameters to be used in track length selection.

Figure 1 shows a cross section of the geometric model used to describe the SNAP-2 LiH shield surrounded by a 20-in.-thick oil-filled collar. The LiH shield is bounded by the z = 0 plane, an ellipsoid approximating the actual toroid, labelled as surface 1 in Fig. 1 a cone (labelled as 2), and a sphere (labelled as 3). The equations of the latter three surfaces are:

1. $x^2 + y^2 + 6.04386(z - 10.3464)^2 - (29.786)^2 = 0$
2. $x^2 + y^2 - 0.021424(z + 189.3257)^2 = 0$
3. $x^2 + y^2 + z^2 - (63.5)^2 = 0.$

The collar itself is bounded by planes at $x = \pm 60.96$, $y = \pm 60.96$, $z = 0$, $z = 50.8$ and the cone describing the side of the LiH shield. Figs. 2 and 3 show cross sections of the models used to describe the other two collars used in the calculations. The collar shown in Fig. 2 has 10 in. of iron followed by 10 in. of transformer oil. The collar shown in Fig. 3 has 4 in. iron, 1 in. oil, 3 in. iron, 2 in. oil, 2 in. iron, 3 in. oil, 1 in. iron, and 4 in. oil, starting at the side nearer the source.

Measurements of fast-neutron dose as a function of distance along the beam centerline indicated that the beam could be described fairly well by a point source emitting particles with a specified angular distribution.

Table I. Experimental Data From Reference 2 Transformed to Equivalent Fast-Neutron Dose Due to Neutrons Leaving the LiH and Collar Shield Surfaces

Collar Description	Angle Between Beam and LiH Shield Centerlines (degrees)	Horizontal Distance* (inches)	Dose Due to Neutrons Leaving LiH Shield Surface ($ergs \cdot gm^{-1} \cdot hr^{-1} \cdot w^{-1}$)	Dose Due to Neutrons Leaving Collar Shield Surface ($ergs \cdot gm^{-1} \cdot hr^{-1} \cdot w^{-1}$)
All Oil	0	0	7.08(-8)**	1.84(-8)
		6	9.00(-8)	3.51(-8)
		12	1.33(-7)	1.27(-7)
		18	2.34(-7)	3.73(-7)
Alternating 1-in. Layer of Iron and Oil	0	0	7.03(-8)	1.32(-8)
		6	8.45(-8)	2.87(-8)
		12	1.06(-7)	1.70(-8)
		18	3.02(-8)	5.70(-8)
	25	0	2.99(-8)	1.43(-8)
		6	3.82(-8)	4.78(-8)
		12	3.39(-8)	6.14(-8)
		18	1.30(-8)	3.76(-8)
4-in. Fe, 1-in. Oil 3-in. Fe, 2-in. Oil 2-in. Fe, 3-in. Oil 1-in. Fe, 4-in. Oil	0	0	7.13(-8)	1.45(-8)
		6	8.10(-8)	2.56(-8)
		12	1.11(-7)	4.57(-8)
		18	2.90(-8)	5.65(-8)
	25	0	2.94(-8)	1.22(-8)
		6	3.66(-8)	4.36(-8)
		12	2.90(-8)	5.60(-8)
		18	9.40(-9)	3.05(-8)

Table I (cont.)

Collar Description	Angle Between Beam and LiH Shield Centerlines (degrees)	Horizontal Distance* (inches)	Dose Due to Neutrons Leaving LiH Shield Surface ($ergs \cdot gm^{-1} \cdot hr^{-1} \cdot w^{-1}$)	Dose Due to Neutrons Leaving Collar Shield Surface ($ergs \cdot gm^{-1} \cdot hr^{-1} \cdot w^{-1}$)
10-in. Fe 10-in. Oil	0	0	7.20(-8)	1.44(-8)
		6	9.39(-8)	2.57(-8)
		12	9.19(-8)	4.51(-8)
		18	2.89(-8)	5.40(-8)
	25	0	2.81(-8)	1.54(-8)
		6	3.34(-8)	4.56(-8)
		12	2.88(-8)	5.81(-8)
		18	7.80(-9)	3.26(-8)
	45	0	1.06(-8)	1.28(-8)
		6	1.18(-8)	2.37(-8)
		12	7.00(-9)	2.75(-8)
		18	3.20(-9)	1.54(-8)

*Horizontal distance between the axis of the neutron beam and the axis of the LiH shield.

**Read 7.08×10^{-8}, etc.

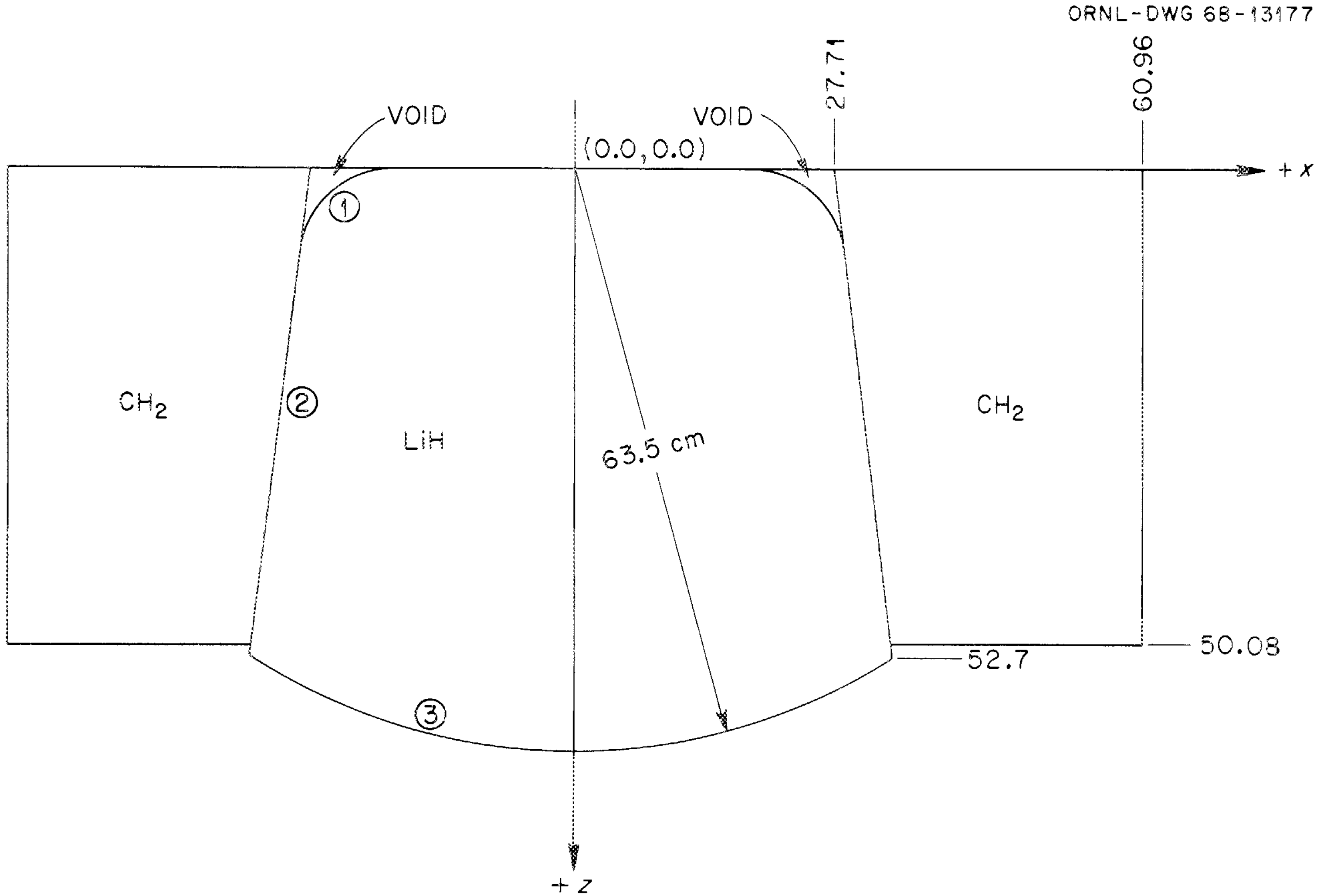

Fig. 1. LiH Shield with CH_2 Collar.

ORNL-DWG 68-13178

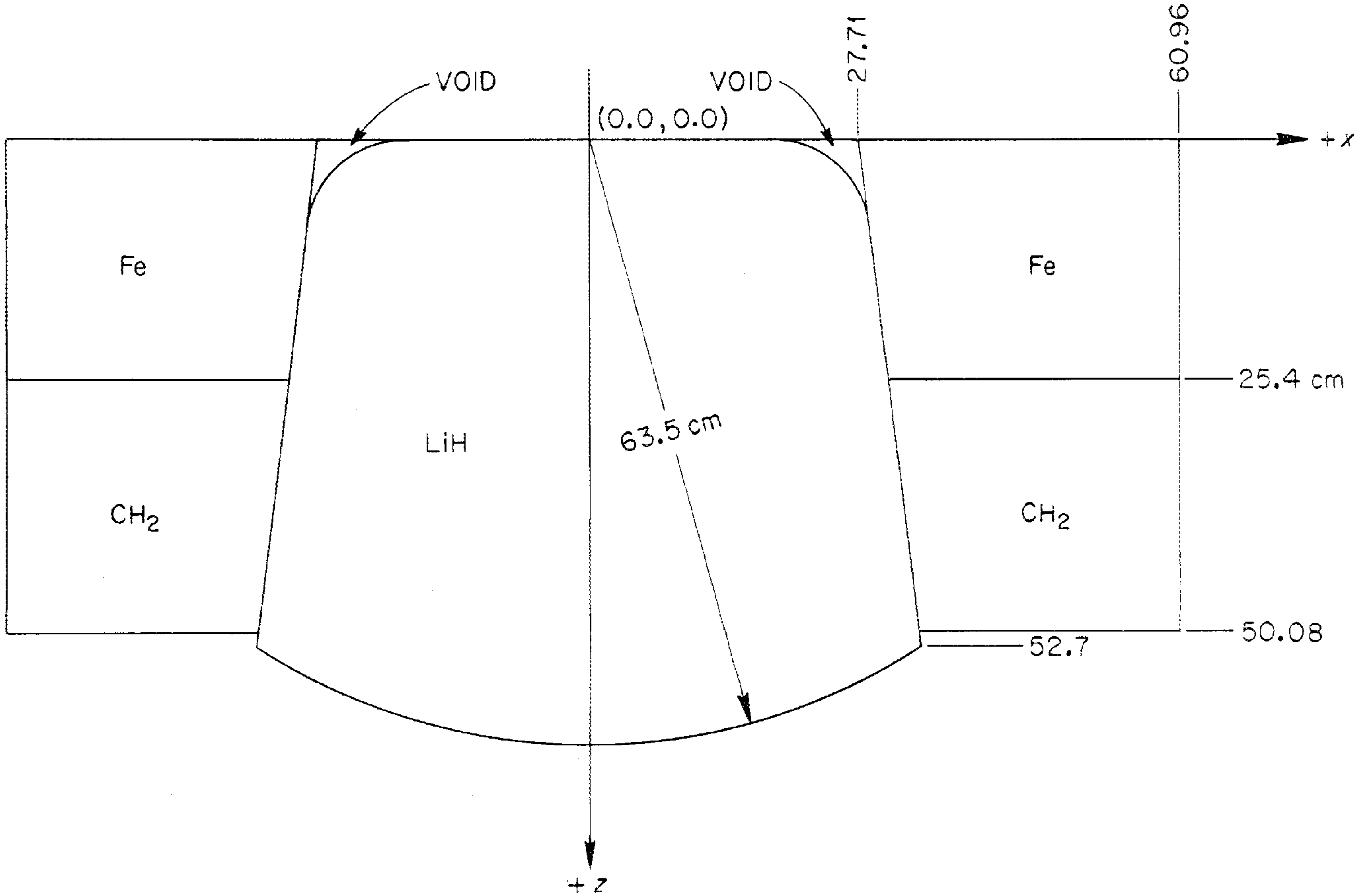

Fig. 2. LiH Shield with 10-in. Fe, 10-in. CH_2 Collar.

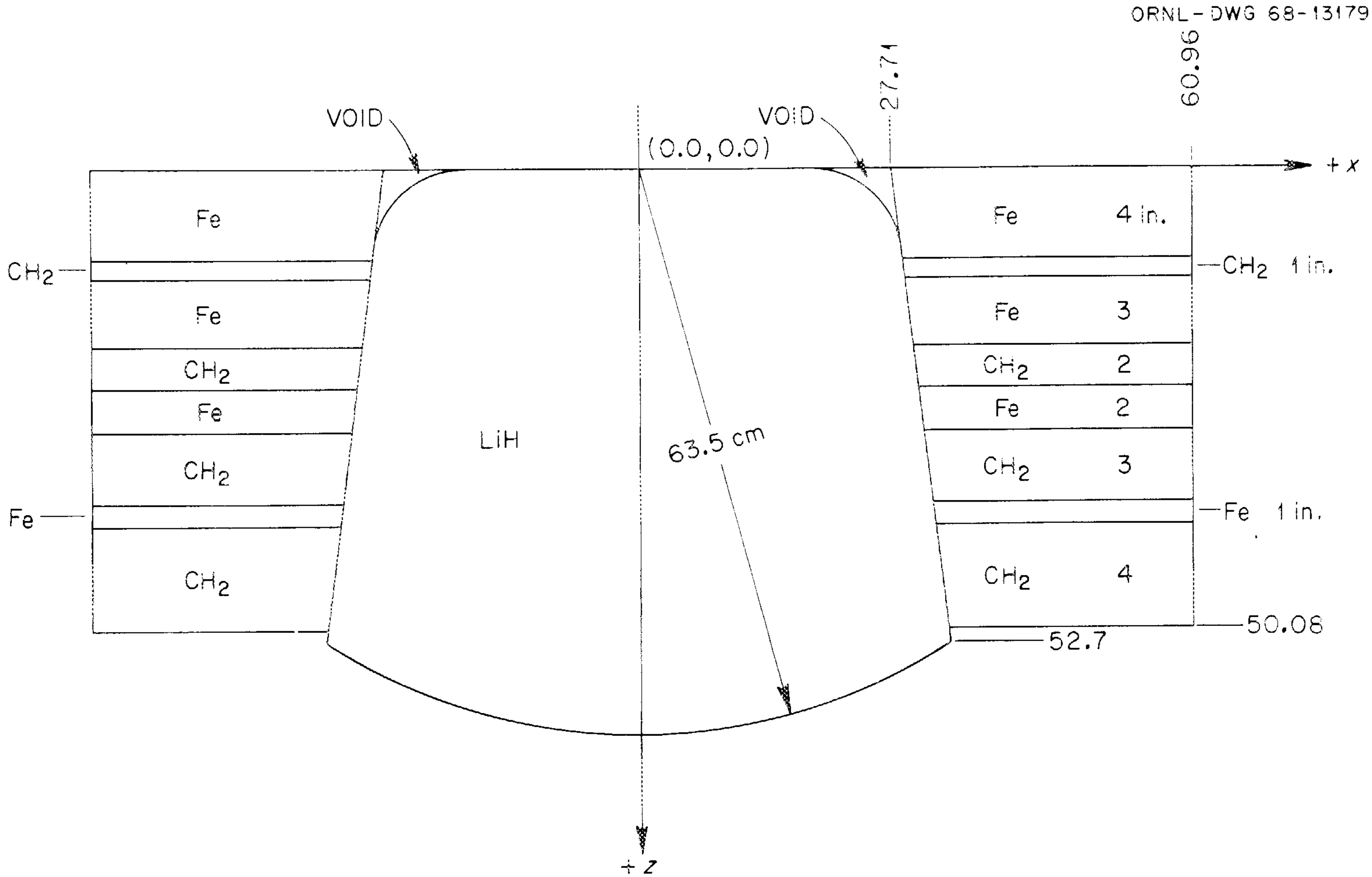

Fig. 3. LiH Shield with Fe, CH_2 Alternating in Unequal Amounts.

The measurements along the centerline were used to locate the point from which the dose varied as $1/r^2$. Traverses across the beam were then used to determine an angular distribution for the point source (Table 8, ref. 2). The distribution which was used, in terms of the cumulative distribution function, is shown in Table II.

The nuclear reactions which were allowed in the LiH were H, ^{6}Li, and ^{7}Li elastic scattering, and ^{6}Li(n,n'), ^{7}Li(n,n'), ^{6}Li(n,dn), and ^{7}Li(n,tn) inelastic scattering. The reactions accounted for in the collar shields were H, ^{12}C, and ^{56}Fe elastic scattering, and ^{12}C(n,n') and ^{56}Fe(n,n') inelastic scattering. The atomic densities of the above nuclides are given in Table III.

III. BIASING

In order to reduce the sample variance in the calculations, several types of biasing were used. The simplest of these was biasing of the source energy. The biasing parameters used, which were determined through trial and error,* are given in Table IV. In each of the energy ranges shown, the density was obtained from prior measurements of the neutron spectrum in the beam.[5]

In addition, track length selection was biased by use of an exponential transform[6] of the form[7]

$$E(\lambda) = \frac{\Sigma_t}{B} e^{-(\Sigma_t/B)\lambda} ,$$

where

*Subsequent work has shown that much better values for these parameters can be obtained from approximate calculations of the value function.

Table II. Angular Distribution Used in the Source Description For All Cases

Cosine Angle From the Beam Centerline	Cumulative Distribution Function
.9453729	0.0
.9503089	.00528007
.9550641	.01085991
.9596285	.01674334
.9639925	.02292451
.9681469	.02944893
.9720821	.03638704
.9757895	.04375844
.9792603	.05153359
.9824865	.05980282
.9854601	.06901063
.9881738	.08050952
.9906212	.10023518
.9927955	.14127605
.9946917	.22555770
.9963047	.36177644
.9976303	.53696470
.9986649	.71968062
.9994063	.87104701
.9998514	.96719557
1.0	1.0

Table III. Atomic Densities of the Nuclides Used in LiH and Collar Shields

Media	Nuclides	Atomic Densities
LiH	^{6}Li	$.00458 \times 10^{24}$
	^{7}Li	$.05416 \times 10^{24}$
	H	$.05874 \times 10^{24}$
CH_2	^{12}C	$.0408 \times 10^{24}$
	H	$.0816 \times 10^{24}$
Fe	^{56}Fe	$.08413 \times 10^{24}$

Table IV. Biasing Used With the Tower Beam Energy Spectrum

Energy Range MeV	Percentage of Neutrons Selected in Energy Range
.2 - 3.0	30%
3.0 - 6.0	35%
6.0 - 9.0	30%
9.0 -	5%

Σ_t = total macroscopic cross section,

λ = path length,

$B = \frac{1}{1 - \nu\omega}$,

ν = biasing parameter, $0 \leqq \nu < 1$,

ω = direction cosine of the neutron velocity, relative to a specified preferred direction.

This form of the exponential transform assumes that the importance function varies exponentially along the preferred direction. From this it can be shown that the proper value of the biasing parameter ν is given by the ratio of the slope of the importance function to the macroscopic cross section. The biasing parameters were given as a function of spatial regions, shown in Fig. 4, and of broad energy groups. The preferred direction was toward +z for regions 1, 2, and 6 through 9 and was normal to the spherical boundaries of regions 3, 4, and 5. The values which were used are given in Table V. They were obtained by adjoint S_n calculations[8] performed with the ANISN code.[9]

The track length selection was also biased to not allow leakage from the system for flights with a positive z-direction cosine.[10]

IV. RESULTS

Twelve of the configurations measured experimentally were used in the calculations. The source descriptions and results for these twelve cases are given in Table VI. The first two data columns give the uncollided and unshielded (the answer that would be obtained without the shield present) flux (n/cm^2) and dose (ergs/gm). The next column gives results for a vacuum replacing the collar. The next column gives results for the

ORNL-DWG 68-13180

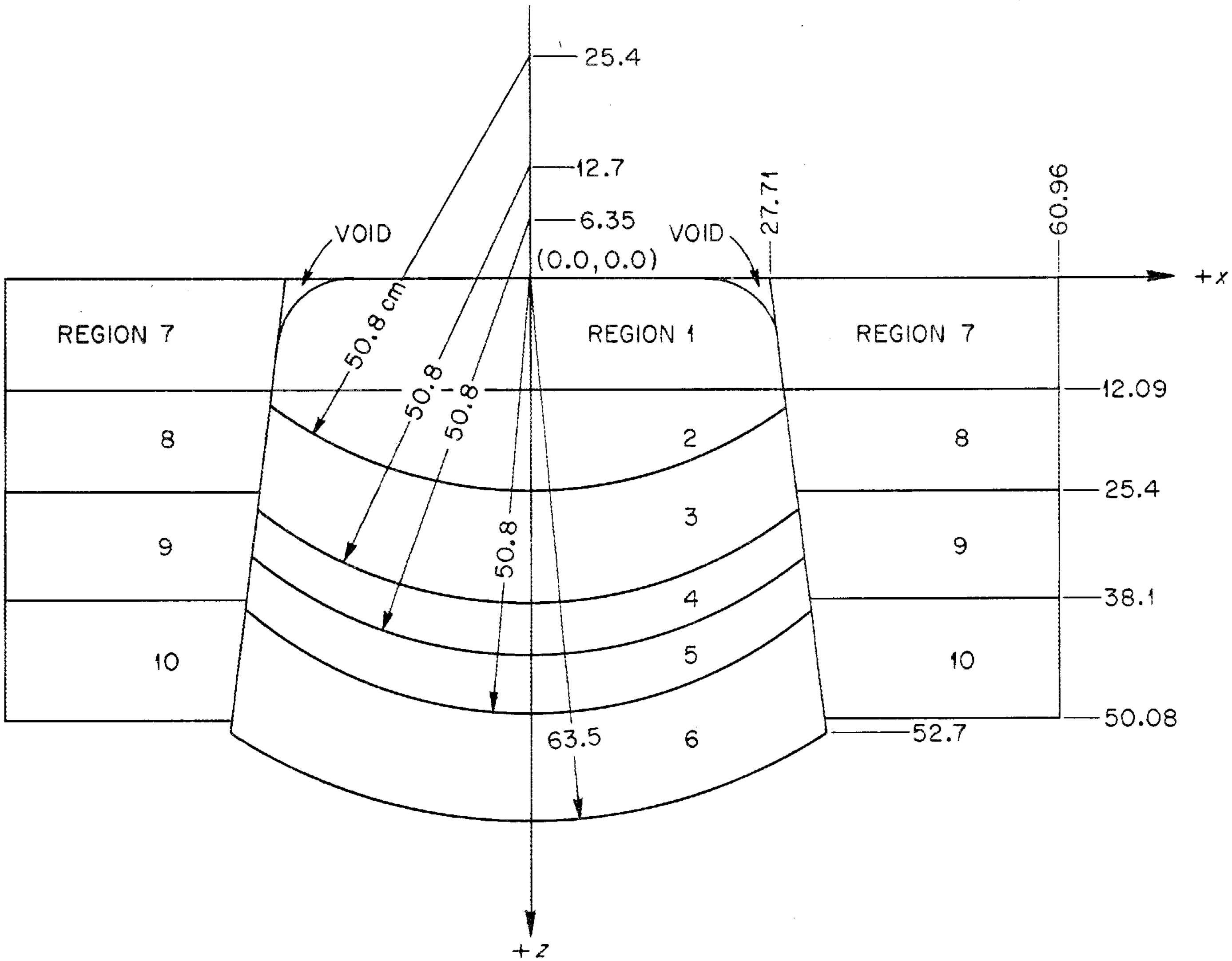

Fig. 4. Region Geometry for LiH Shield and Collar Shield.

Table V. Energy and Region Dependent Preferred Track Direction Biasing Factors

Energy (Speed-Squared Units) \ Region No.	1	2	3	4	5	6
6.41×10^{15}	.482	.482	.482	.481	.479	.465
2.87×10^{16}	.590	.591	.593	.599	.621	.685
2.12×10^{17}	.828	.828	.827	.824	.812	.647
7.8×10^{17}	.983	.972	.951	.919	.872	.557
1.16×10^{18}	.955	.941	.911	.867	.802	.419
1.74×10^{18}	.965	.944	.903	.846	.767	.337
2.12×10^{18}	.951	.927	.880	.817	.732	.281
2.58×10^{18}	.936	.909	.848	.790	.700	.231
3.16×10^{18}	.919	.889	.834	.763	.669	.188
3.86×10^{18}	.902	.870	.812	.738	.640	.148
4.71×10^{18}	.889	.855	.794	.716	.614	.105
5.76×10^{18}	.873	.837	.774	.694	.589	.068
7.04×10^{18}	.862	.825	.759	.675	.566	.023
8.61×10^{18}	.855	.815	.746	.656	.539	0.0
1.05×10^{18}	.846	.805	.731	.634	.509	0.0
1.28×10^{18}	.836	.792	.712	.608	.471	0.0
1.56×10^{18}	.819	.772	.685	.571	.421	0.0
1.91×10^{18}	.790	.738	.644	.519	.355	0.0
2.33×10^{19}	.744	.688	.584	.447	.266	0.0

Table VI. Source Descriptions and Results of O5R Calculations

Collar Description	Angle Between Beam Centerline and Shield Centerline	Point Source Location (x,y,z) cm	Horizontal Distance (inches)	Flux (above) and Dose (below) for 10,000 Source Particles				
				Uncollided	Unshielded	Due to Neutrons Never Leaving LiH Shield	Due to Neutrons Leaving Lih Shield Surface	Due to Neutrons Leaving Collar Shield Surface
All Oil	0°	(-15.24,0.0,-147.32)	6	1.01 (-6) 1.75 (-11)	7.50 (-1) 8.17 (-6)	2.50 (-6) 3.24 (-11)	2.87 (-6) 3.67 (-11)	1.58 (-6) 2.04 (-11)
		(-30.48,0.0,-147.32)	12	2.45 (-6) 4.18 (-11)	7.00 (-1) 7.61 (-6)	1.68 (-6) 2.36 (-11)	2.90 (-6) 4.12 (-11)	4.98 (-6) 6.93 (-11)
4-in. Fe, 1-in. Oil 3-in. Fe, 2-in. Oil	0°	(-15.24,0.0,-147.32)	6	9.75 (-7) 1.68 (-11)	7.54 (-1) 8.22 (-6)	1.96 (-6) 2.70 (-11)	2.40 (-6) 3.16 (-11)	5.79 (-7) 6.84 (-12)
2-in. Fe, 3-in. Oil 1-in. Fe, 4-in. Oil		(-30.48,0.0,-147.32)	12	2.54 (-6) 4.34 (-11)	6.98 (-1) 7.60 (-6)	1.40 (-6) 2.05 (-11)	2.20 (-6) 3.21 (-11)	2.12 (-6) 2.36 (-11)
10-in. Fe, 10-in. Oil	0°	(0.,0.0,-147.32)	0	9.43 (-7) 1.65 (-11)	7.56 (-1) 8.25 (-6)	1.83 (-6) 2.47 (-11)	2.16 (-6) 2.94 (-11)	1.97 (-7) 6.13 (-11)
		(-15.24,0.0,-147.32)	6	1.06 (-6) 1.84 (-11)	7.47 (-1) 8.17 (-6)	2.57 (-6) 3.48 (-11)	2.76 (-6) 3.71 (-11)	1.39 (-6) 1.86 (-11)
		(-30.48,0.0,-147.32)	12	2.50 (-6) 4.26 (-11)	6.97 (-1) 7.61 (-6)	1.25 (-6) 1.72 (-11)	2.03 (-6) 2.77 (-11)	6.73 (-6) 6.81 (-11)
	25°	(-62.26,0.0,-133.518)	0			1.27 (-6) 1.65 (-11)	1.39 (-6) 1.82 (-11)	1.04 (-6) 1.34 (-11)
		(-47.02,0.0,-133.518	6			7.88 (-7) 1.06 (-11)	1.46 (-6) 1.92 (-11)	1.04 (-6) 1.24 (-11)
		(-31.78,0.0,-133.518)	12			3.77 (-7) 4.80 (-12)	7.87 (-7) 1.04 (-11)	1.80 (-6) 2.24 (-11)
	45°	(-104.171,0.0,-104.171)	0			4.14 (-7) 4.93 (-12)	4.68 (-7) 5.63 (-12)	5.63 (-7) 6.80 (-12)
		(-88.93,0.0,-104.171)	6			2.27 (-7) 3.08 (-12)	3.24 (-7) 4.39 (-12)	2.31 (-6) 2.74 (-11)

case of the collar present and assuming perfect detector collimation so that only the particles leaving the LiH shield surface are detected. The last column gives flux and dose due to the particles leaving the collar shield surface.

Comparison of experimental and calculated results are given in Table VII. All results are dose at the detector per unit dose incident on the shield. The experimental results were taken from Table I and were divided by the 168.6 $erg \cdot gm^{-1} \cdot hr^{-1} \cdot w^{-1} \cdot cm^{2}$ incident on the shield (units of Table I are $erg \cdot gm^{-1} \cdot hr^{-1} \cdot w^{-1}$). The calculated results in Table VI were divided by the 10^{4} source neutrons and the dose per source neutron: 1.039×10^{-5} $erg \cdot gm^{-1} \cdot source\ neutron^{-1}$.

The comparison of calculated and experimental results can be seen to be quite good in most cases. For fifteen of the twenty-four cases, the measurement can be seen to be within 1 standard deviation (statistical deviation in the calculations) of the corresponding calculation.

Table VII. Comparison of Experimental and Calculated Dose Rates Due to Neutrons Leaving the LiH Shield Surface and the Collar Shield Surface

Collar Description	Angle Between Beam and LiH Shield Centerlines	Horizontal Distance (inches)	Dose Due to Neutrons Leaving LiH Shield Surface		Dose Due to Neutrons Leaving Collar Shield Surface	
			Calculated	Measured	Calculated	Measured
All Oil	0^{o}	6	5.22 (-10) (.08)	5.34 (-10)	1.97 (-10) (.29)	2.08 (-10)
		12	8.0 (-10) (.08)	7.89 (-10)	6.67 (-10) (.12)	7.53 (-10)
4-in. Fe, 1-in. Oil	0^{o}	6	4.66 (-10) (.11)	4.8 (-10)	6.58 (-11) (.21)	1.52 (-10)
3-in. Fe, 2-in. Oil						
2-in. Fe, 3-in. Oil		12	7.27 (-10) (.11)	6.58 (-10)	2.27 (-10) (.41)	2.71 (-10)
1-in. Fe, 4-in. Oil						
10-in. Fe	0^{o}	0	4.42 (-10) (.11)	4.27 (-10)	5.9 (-11) ((.43)	8.54 (-11)
10-in. Oil		6	5.34 (-10) (.07)	5.57 (-10)	1.79 (-10) (.46)	1.52 (-10)
		12	6.78 (-10) (.11)	5.45 (-10)	6.55 (-10) (.63)	2.67 (-10)
	25^{o}	0	1.75 (-10) (.12)	1.67 (-10)	1.29 (-10) (.61)	9.13 (-11)
		6	1.85 (-10) (.13)	1.98 (-10)	1.19 (-10) (.16)	2.7 (-10)
		12	1.00 (-10) (.13)	1.71 (-10)	2.16 (-10) (.14)	3.44 (-10)
	45^{o}	0	5.42 (-11) (.14)	6.29 (-11)	6.54 (-11) (.48)	7.6 (-11)
		6	4.23 (-11) (.19)	7.0 (-11)	2.64 (-10) (.59)	1.4 (-10)

REFERENCES

1. F. H. S. Clark, F. B. K. Kam, and N. A. Betz, Neutron Phys. Div. Ann. Progr. Rept. Aug. 1, 1963, ORNL-3499, Vol. I, p. 116.
2. F. J. Muckenthaler, "Comparison of Monte Carlo Calculations with Measurements of Fast Neutron Dose Transmitted from a Beam Source Through a SNAP-2 LiH Shield."
3. D. C. Irving, R. M. Freestone, Jr., and F. B. K. Kam, O5R, A General-Purpose Monte Carlo Transport Code, ORNL-3622 (1965).
4. F. B. K. Kam and K. D. Franz, ACTIFK, A General Analysis Code for O5R, ORNL-3856 (1966).
5. F. B. K. Kam, Personal Communication.
6. F. H. Clark, The Exponential Transform as an Importance-Sampling Device - A Review, ORNL-RSIC-14 (1966).
7. V. R. Cain, E. A. Straker, and G. Thayer, Monte Carlo Path Selection Routines Based on Some Specific Forms of the Importance Function, ORNL-TM-1967 (to be published).
8. R. R. Coveyou, V. R. Cain, and K. J. Yost, "Adjoint and Importance in Monte Carlo Application," ORNL-4093 (1967).
9. W. W. Engle, "A User's Manual for ANISN, A One-Dimensional Discrete Ordinates Transport Code With Anisotropic Scattering," K-1693 (1967).
10. F. H. Clark and N. A. Betz, Importance Sampling Device for Selecting Track Lengths and Directions After Scatter in O5R, ORNL-TM-1484 (1966).

INTERNAL DISTRIBUTION

1- 3. L. S. Abbott
4. R. S. Booth
5-14. V. R. Cain
15-19. C. E. Clifford
20-29. K. D. Franz
30. J. Lewin
31. R. E. Maerker
32-33. F. C. Maienschein
34. F. J. Muckenthaler
35. F. R. Mynatt
36. S. K. Penny
37. E. A. Straker
38. D. Sundberg
39. D. K. Trubey
40. K. J. Yost
41. E. R. Cohen (consultant)
42. B. C. Diven (consultant)
43. W. N. Hess (consultant)
44. M. H. Kalos (consultant)
45. L. V. Spencer (consultant)
46-47. Central Research Library
48. ORNL Y-12 Technical Library Document Reference Section
49-50. Laboratory Records Dept.
51. Laboratory Records ORNL RC
52. ORNL Patent Office

EXTERNAL DISTRIBUTION

53. P. B. Hemmig, Division of Reactor Development and Technology, U. S. Atomic Energy Commission, Washington, D. C.
54. I. F. Zartman, Division of Reactor Development and Technology, U. S. Atomic Energy Commission, Washington, D. C.
55-69. Division of Technical Information Extension (DTIE)
70. Laboratory and University Division (ORO)
71. Dr. J. R. Beyster, Gulf General Atomic, Inc., P. O. Box 608, San Diego, California 92112
72. Mr. Robert L. Detterman, Atomics International, 8900 Desota Street, Box 309, Canoga Park, California
73. Capt. R. W. Enz, Department of Defense, Defense Atomic Support Agency, Washington, D. C. 20305
74. Mr. Joseph G. Gallagher, Manager, Thermal and Nuclear Design, Westinghouse Astronuclear Laboratory, P. O. Box 10864, Pittsburgh, Pennsylvania 15236
75. Dr. Glen A. Graves, N-2 Division, Los Alamos Scientific Laboratory, P. O. Box 1663, Los Alamos, New Mexico 87544
76. Mr. Paul G. Johnson, Space Nuclear Propulsion Office, U. S. Atomic Energy Commission, Washington, D. C. 20545
77. Mr. Irving M. Karp, Lewis Research Center, National Aeronautics and Space Administration, 21000 Brookpark Road, Cleveland, Ohio 44135
78. Capt. G. Kerley, Department of Defense, Defense Atomic Support Agency, Washington, D. C. 20305
79. Mr. C. P. McCallum, Division of Space Nuclear Systems, U. S. Atomic Energy Commission, Washington, D. C. 20546

80. Lt. Col. G . C. Reinhardt, Department of Defense, Defense Atomic Support Agency, Washington, D. C. 20305

81. Mr. E. A. Warman, Nuclear Rocket Operations, Aerojet-General Corporation, Dept. 7850, Bldg. 2019, P. O. Box 15847, Sacramento, California 95813